

## A Microphone Array Method Benchmarking Exercise using Synthesized Input Data

Sarradj, Ennes; Herold, Gert; Sijtsma, Pieter; Merino Martinez, Roberto; Malgoezar, Anwar; Snellen, Mirjam; Geyer, Thomas F.; Bahr, Christopher J.; Porteous, Ric; Moreau, Danielle J.

**DOI**

[10.2514/6.2017-3719](https://doi.org/10.2514/6.2017-3719)

**Publication date**

2017

**Document Version**

Accepted author manuscript

**Published in**

23rd AIAA/CEAS Aeroacoustics Conference

**Citation (APA)**

Sarradj, E., Herold, G., Sijtsma, P., Merino Martinez, R., Malgoezar, A., Snellen, M., Geyer, T. F., Bahr, C. J., Porteous, R., Moreau, D. J., & Doolan, C. J. (2017). A Microphone Array Method Benchmarking Exercise using Synthesized Input Data. In *23rd AIAA/CEAS Aeroacoustics Conference: 5-9 June 2017, Denver, Colorado* Article AIAA 2017-3719 American Institute of Aeronautics and Astronautics Inc. (AIAA). <https://doi.org/10.2514/6.2017-3719>

**Important note**

To cite this publication, please use the final published version (if applicable). Please check the document version above.

**Copyright**

Other than for strictly personal use, it is not permitted to download, forward or distribute the text or part of it, without the consent of the author(s) and/or copyright holder(s), unless the work is under an open content license such as Creative Commons.

**Takedown policy**

Please contact us and provide details if you believe this document breaches copyrights. We will remove access to the work immediately and investigate your claim.

# A microphone array method benchmarking exercise using synthesized input data

Ennes Sarradj<sup>\*</sup> and Gert Herold<sup>†</sup>

*Technische Universität Berlin, 10587 Berlin, Germany*

Pieter Sijtsma<sup>‡</sup>

*PSA3, 8091 AV Wezep, The Netherlands*

Roberto Merino-Martinez<sup>§</sup>, Anwar Malgoezar<sup>§</sup> and Mirjam Snellen<sup>¶</sup>

*Delft University of Technology, 2629 HS Delft, The Netherlands*

Thomas F. Geyer<sup>||</sup>

*Brandenburg University of Technology Cottbus - Senftenberg, 03046 Cottbus, Germany*

Christopher J. Bahr<sup>\*\*</sup>

*NASA Langley Research Center, Hampton, Virginia 23681*

Ric Porteous<sup>††</sup>

*The University of Adelaide, Adelaide, South Australia 5005, Australia*

Danielle J. Moreau<sup>‡‡</sup> and Con J. Doolan<sup>§§</sup>

*The University of New South Wales, Sydney NSW 2052, Australia*

---

<sup>\*</sup>Professor, Institute of Fluid Mechanics and Engineering Acoustics, [ennes.sarradj@tu-berlin.de](mailto:ennes.sarradj@tu-berlin.de)

<sup>†</sup>PhD student, Institute of Fluid Mechanics and Engineering Acoustics, [gert.herold@tu-berlin.de](mailto:gert.herold@tu-berlin.de)

<sup>‡</sup>Director; also at Aircraft Noise & Climate Effects, Delft University of Technology, Faculty of Aerospace Engineering, The Netherlands, [pieter.sijtsma@psa3.nl](mailto:pieter.sijtsma@psa3.nl)

<sup>§</sup>PhD candidates, Aircraft Noise & Climate Effects Section, Faculty of Aerospace Engineering, [R.MerinoMartinez@tudelft.nl](mailto:R.MerinoMartinez@tudelft.nl) and [A.M.N.Malgoezar@tudelft.nl](mailto:A.M.N.Malgoezar@tudelft.nl)

<sup>¶</sup>Associate Professor, Aircraft Noise & Climate Effects Section, Faculty of Aerospace Engineering, [M.Snellen@tudelft.nl](mailto:M.Snellen@tudelft.nl)

<sup>||</sup>Research Associate, Chair of Technical Acoustics, [thomas.geyer@b-tu.de](mailto:thomas.geyer@b-tu.de)

<sup>\*\*</sup>Research Engineer, Aeroacoustics Branch, Senior Member AIAA, [christopher.j.bahr@nasa.gov](mailto:christopher.j.bahr@nasa.gov)

<sup>††</sup>Ph.D. Candidate, School of Mechanical Engineering, [ric.porteous@adelaide.edu.au](mailto:ric.porteous@adelaide.edu.au)

<sup>‡‡</sup>Lecturer, School of Mechanical and Manufacturing Engineering, Member AIAA, [d.moreau@unsw.edu.au](mailto:d.moreau@unsw.edu.au)

<sup>§§</sup>Associate Professor, School of Mechanical and Manufacturing Engineering, Senior Member AIAA, [c.doolan@unsw.edu.au](mailto:c.doolan@unsw.edu.au)

## I. Introduction

Microphone arrays are widely used for aeroacoustic testing. A great variety of approaches exists to collect and process the data from measurements with microphone arrays. Different beamforming algorithms, deconvolution and other processing methods are applied. On many occasions, it has turned out that it is necessary to have a better assessment of these methods. The microphone array community agreed on starting an effort to test and analyze microphone array methods using a set of common data sets.

In this contribution, two of these data sets are considered that are both based not on measured, but on synthesized input data. One of these data sets concerns a group of four point sources; the other is focused on a line source. Synthesized data provide an advantage over experimental data when analyzing methods, as the correct solution is known. This allows the study of possible errors produced by the individual methods. A companion paper<sup>1</sup> addresses two experimental data sets from the same benchmark effort.

## II. Participants and processing methods

The following research groups or individuals have participated and have delivered results for at least one of the two analytical benchmarks:

- NASA Langley Research Center, Aeroacoustics Branch, United States (NASA),
- Brandenburg University of Technology Cottbus - Senftenberg and TU Berlin, Institute of Fluid Mechanics and Engineering Acoustics, Germany (BTU),
- PSA3, the Netherlands (PSA3),
- Delft University of Technology, Aircraft Noise & Climate Effects Section, Faculty of Aerospace Engineering, the Netherlands (TUD),
- The University of Adelaide, School of Mechanical Engineering and The University of New South Wales, School of Mechanical and Manufacturing Engineering, Australia (UniA).

Generally, each contributing group used their own in-house implementation of the microphone array methods. In the contributions from BTU, a freely available open-source code was used.<sup>2</sup>

A number of different processing methods were applied in the benchmark exercise. All methods are based on the cross spectral matrix (CSM) of the microphone signals and thus, work in the frequency domain. Some of them are based on Conventional Beamforming, where steering vectors are pre- and post-multiplied to the CSM to spatially filter out sources on a given grid. The extension and spatial resolution of this grid are parameters that are relevant to the performance.

The following methods were tested:

**DAMAS**<sup>3</sup> DAMAS aims at solving the convolution equation by a Gauss-Seidel procedure, replacing non-physical negative solutions by zero. Two partners (BTU and NASA) tested their DAMAS codes. NASA applied DAMAS at three different settings: without CSM diagonal removal, with diagonal removal, and with an eigenvalue based diagonal reconstruction procedure. DAMAS requires specifying both the order in which the Gauss-Seidel system is evaluated (grid sweep order) and the number of iterations of the Gauss-Seidel procedure.

**CLEAN-SC**<sup>4</sup> CLEAN-SC basically performs a decomposition of the CSM into coherent components. Unlike other deconvolution methods, it does not use the Point Spread Function. It works well in combination with CSM diagonal removal. CLEAN-SC was tested by PSA3, BTU and UniA. CLEAN-SC takes two parameters: the damping factor and the number of iterations. The latter can also be deduced automatically.

**Orthogonal Beamforming<sup>5</sup> (OB)** This method identifies the signal subspace in the CSM by performing an eigenvalue analysis. The Conventional Beamforming algorithm is applied to the signal-related eigenvectors, which are orthogonal. Thus, high performance in terms of processing speed is achieved. OB was tested by BTU. OB takes one parameter, which is the number of eigenvalues assumed for the signal subspace.

**Functional Beamforming<sup>6</sup> (FB)** FB raises the CSM to the power of  $\frac{1}{\nu}$ , uses the results in the beamforming algorithm, and then raises the beamforming output to the power of  $\nu$ . The result is that side lobes of point spread functions are suppressed, dependent on the exponent. FB does not perform well with diagonal removal, and diagonal reconstruction methods are under investigation. FB was tested by TUD. FB takes one parameter  $\nu \geq 1$ , which is used in the algorithm as described.

**Covariance Matrix Fitting<sup>7</sup> (CMF)** The idea of CMF is to minimize, in terms of least squares, the difference between the “measured” CSM and the CSM that would be obtained with a set of uncorrelated sources of equal strength. This optimization can be done without the diagonal of the CSM. There are different types of this method, depending on what sources are assumed and what solution strategy is applied. CMF was tested by BTU, where point sources were assumed and a non-negative least squares (NNLS) solver was used to solve the system.

**Source Power Integration<sup>8</sup> (SPI)** SPI is a summation over Conventional Beamforming results, scaled by means of a source in the center of the scan grid or by a group of sources. To avoid side lobes, the summation is usually done with a certain threshold, which is also the only parameter that can be given. SPI was tested by the University of Adelaide. An advanced SPI method was tested by TUD, which assumed the existence of a line source. This is similar to CMF with the assumption of a line source and the use of an explicit solution. No threshold needs to be applied for the advanced SPI.

**Global Optimization<sup>9</sup> (GO)** This method solves essentially the same problem as CMF, but using a global optimization method. The method was tested by TUD, using Differential Evolution as the global optimization method. GO needs no grid, but a number of parameters to constrain the set of possible solutions. In addition, parameters for the optimization method itself have to be set.

Quantitative results can be computed through integration over a sector in the result map. The extension of a sector is another parameter that potentially has an influence on the result.

### III. Case: four point sources

The test case is contributed by BTU and addresses the ability of the microphone array methods to obtain correct source levels for a limited number of sources. The idea is to test whether the different methods are able to do this for sources of known location.

#### A. Case description

The case includes four monopole sources at the corners of an 0.2 m by 0.2 m square. The sources are located at 0.75 m distance (see the coordinates in Table 1) from an array of 64 microphones. The array has a seven arm logarithmic spiral arrangement and an aperture of approximately 1.5 m, see Fig. 1. Two subcases are considered:

**subcase a:** All sources have the same power.

**subcase b:** The sources all have different power. One source has a power level that is approximately 6 dB less than the strongest source. Two more sources have a power approximately 12 dB and 18 dB less than the strongest source, respectively.

For each subcase both time series and the CSM are provided. The source signals are simulated in the time domain as white noise (with a normal distribution of amplitude probability) with a duration of 10 s.

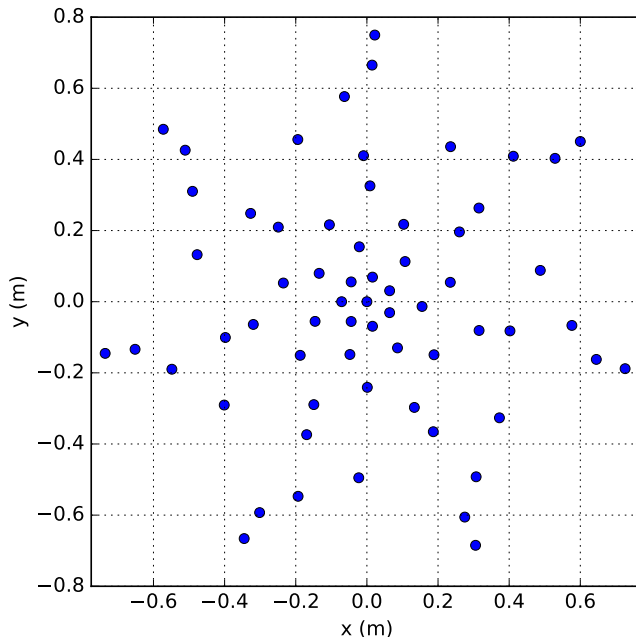


Figure 1. Arrangement of the 64 array microphones.

Independent random number generators with a normal distribution are used for each of the sources. Consequently, the contributions of the individual sources at each of the microphones are uncorrelated. To obtain the microphone signals, the source signals are first delayed by an appropriate amount of time and afterwards they are superposed for each individual microphone. The microphone signals are then sampled with a rate of 51.2 kHz. From the microphone signals, the CSM is computed using 999 frames of 1024 samples each with a Hanning window applied and 50% overlap. The CSM thus contains values for 513 frequencies (multiples of 50 Hz).

## B. Metrics and contributions

The challenge is to obtain the correct value of the source strength measured as sound pressure in the array center. As all methods depend on at least one parameter, it can be expected that these parameters have some influence on the result.

From the first contributions, it became clear that different contributors took very different approaches to parameter selection. In order to make a more meaningful comparison of the results, for some parameters, common values to be used by all participants were suggested. This concerned the grid and some method-specific parameters as shown in Tab. 2. For the estimation of the source strength, a spatial integration over a square with a side length of 0.1 m centered at the nominal source position was suggested. However, not all contributors were able to adapt their computation to this set of parameters.

Because of the limited duration of the white signals, the power spectra are not *perfectly* flat. Therefore, the true values of the auto power spectrum measured in the array center for each source individually are used for comparison to any beamforming results. The level difference

$$\Delta L = L_{\text{estimated}} - L_{\text{true}}$$

between the estimated and the true source level was used as an error metric. In the case of a perfect estimation, this level difference should vanish.

Results were contributed by all five groups and several methods – DAMAS, CLEAN-SC, OB, CMF and GO– were applied to process the data from this case. Tab. 3 gives an overview about all contributions. For all contributions, both subcase a and subcase b were considered.

**Table 1. Locations of the sources with respect to the array center (given in m).**

	$x$	$y$	$z$
source 0	0.1	-0.1	0.75
source 1	-0.1	-0.1	0.75
source 2	-0.1	0.1	0.75
source 3	0.1	0.1	0.75

**Table 2. Suggested method parameters.**

Method	Parameters
grid, all methods	$x_{min} = -0.5, x_{max} = 0.5, y_{min} = -0.5, y_{max} = 0.5, z = 0.75, \text{resolution} = 0.025$
DAMAS	200 iterations
CLEAN-SC	damping 0.9

### C. Results

By all contributors, third-octave band spectra of the source strength were submitted. These results were used to compute the error metric for all sources.

Fig. 2 shows the results for the subcase with four equally strong sources. With two exceptions, all methods deliver results roughly with an error margin of  $\pm 1$  dB. The first exception is OB. One underlying assumption for that method is that the sources have different strengths.<sup>5</sup> Thus, it can be expected that the method has a larger error with multiple equally strong sources. The second exception is GO, that has some larger errors at higher frequencies. This is probably due to the larger number of local optima that can be expected for higher frequencies. Better results could possibly be produced using different optimization methods or parameters for the method.

Another conclusion from the results is that different implementations of the same algorithm can deliver different results. This is obvious when comparing either all CLEAN-SC or all DAMAS results (see Fig. 3). Possible reasons for this behavior are implementation details such as the criterion for stopping the iteration process in CLEAN-SC or the sequence of the direction of iteration passes in DAMAS. Other possible reasons are the different grid resolutions and different steering vectors<sup>10</sup> used in different contributions and the different approaches regarding the CSM diagonal deletion.

Fig. 4 shows the results for the subcase with sources of different strength. For the two strongest sources, all methods work within roughly 1 dB error margin. For the two weaker sources, some of the results show larger deviations or even break down. It seems to be a particular challenge for some implementations to properly estimate weak sources in the presence of much stronger sources. However, this does not seem to be connected to a certain method and instead seems to depend on implementation details.

**Table 3. Overview of contributions for case of four sources (all dimensions in meters).**

Contributor and method	Parameters grid resolution: 0.025 unless otherwise noticed	integration sector centered at nominal source position
NASA DAMAS	number of iteration passes: 200 CSM diagonal removal	square $0.1 \times 0.1$
NASA DAMAS EigDR	number of iteration passes: 200 CSM eigenvalue based diagonal reconstruction	square $0.1 \times 0.1$
NASA DAMAS NoDR	number of iteration passes: 200 no CSM diagonal removal	square $0.1 \times 0.1$
BTU DAMAS	number of iteration passes: 200 CSM diagonal removal	square $0.1 \times 0.1$
UniA DAMAS	no CSM diagonal removal grid resolution: 0.04	square $0.2 \times 0.2$
BTU CLEAN-SC	damping: 0.9 CSM diagonal removal	square $0.1 \times 0.1$
PSA3 CLEAN-SC	damping: 0.9 no CSM diagonal removal grid resolution: 0.01	square $0.1 \times 0.1$
UniA CLEAN-SC	damping: 0.99 no CSM diagonal removal grid resolution: 0.02	square $0.1 \times 0.1$
BTU OB	source count: 16 CSM diagonal removal	square $0.1 \times 0.1$
BTU CMF	solver: NNLS CSM diagonal removal	square $0.1 \times 0.1$
TUD GO	solver: differential evolution number of sources: 4 population size: 128 generations: 600 crossover-rate: 0.4 multiplication factor: 0.75 number of independent runs: 50	circle, radius 0.05

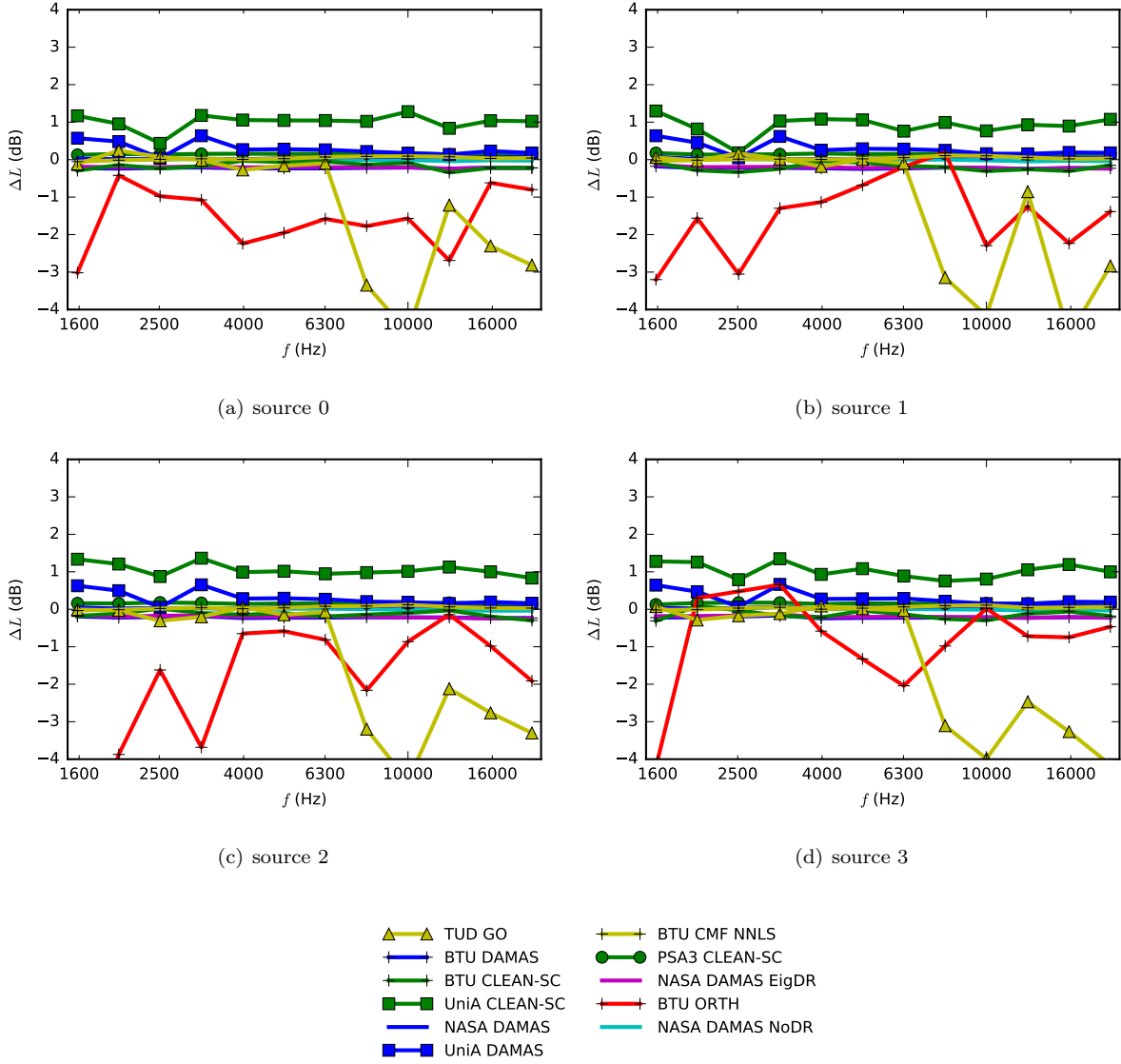
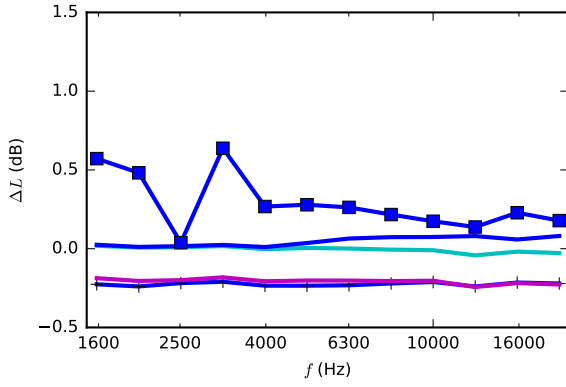
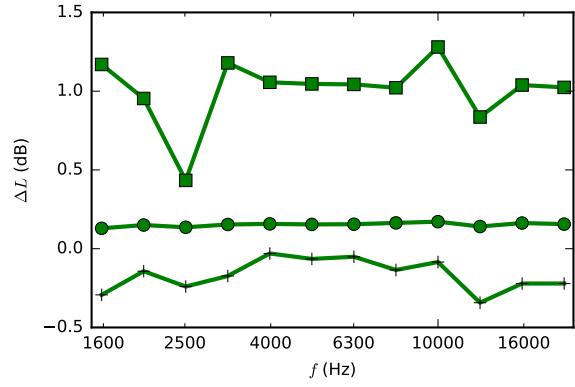


Figure 2. Results for subcase a of the four point source case.

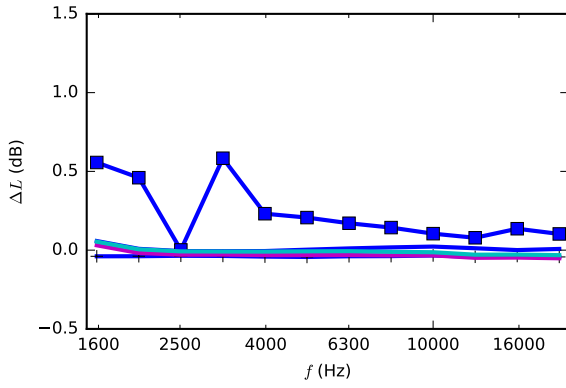




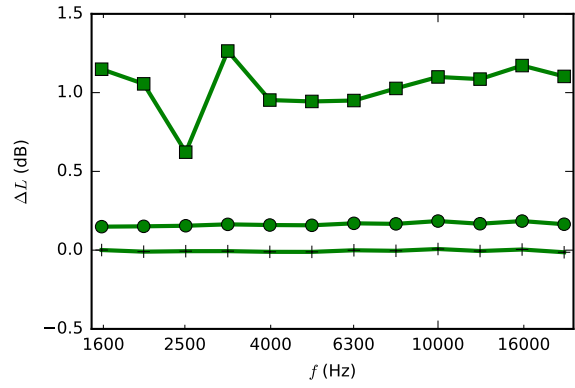
(a) subcase a, source 0, DAMAS results



(b) subcase a, source 0, CLEAN-SC results



(c) subcase b, source 0, DAMAS results



(d) subcase b, source 0, CLEAN-SC results

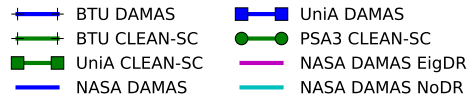
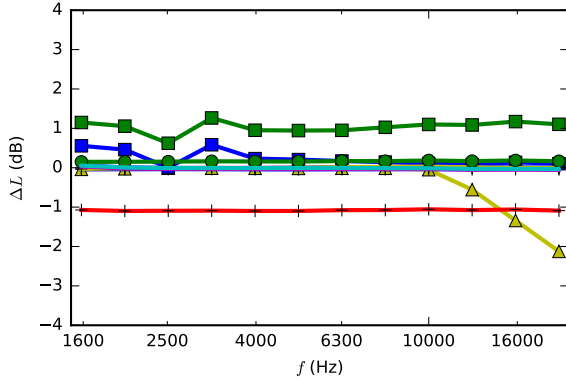
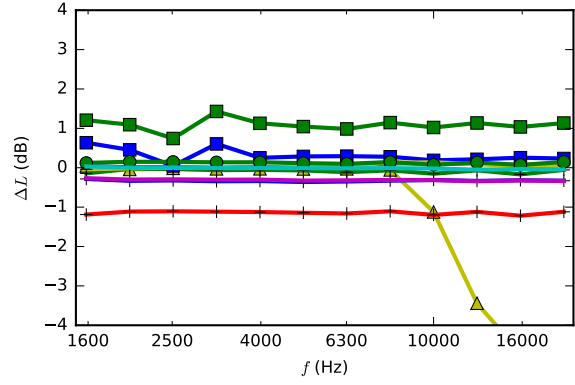


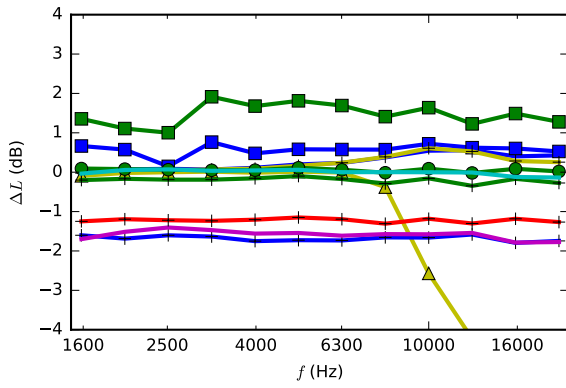
Figure 3. DAMAS and CLEAN-SC results for both subcases of the four point source case.



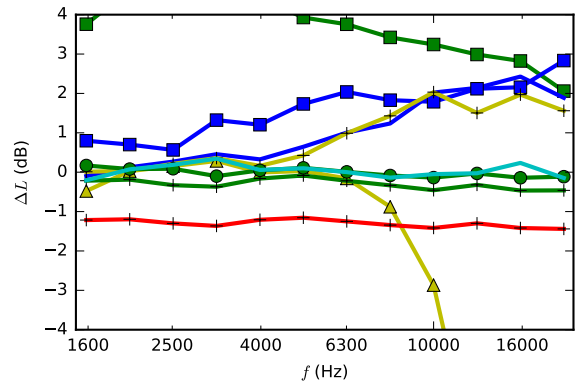
(a) source 0



(b) source 1 (-6 dB)



(c) source 2 (-12 dB)



(d) source 3 (-18 dB)

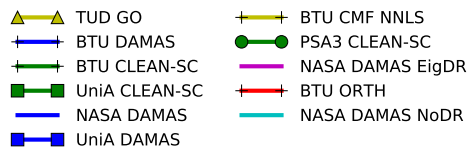


Figure 4. Results for subcase b of the four point source case.

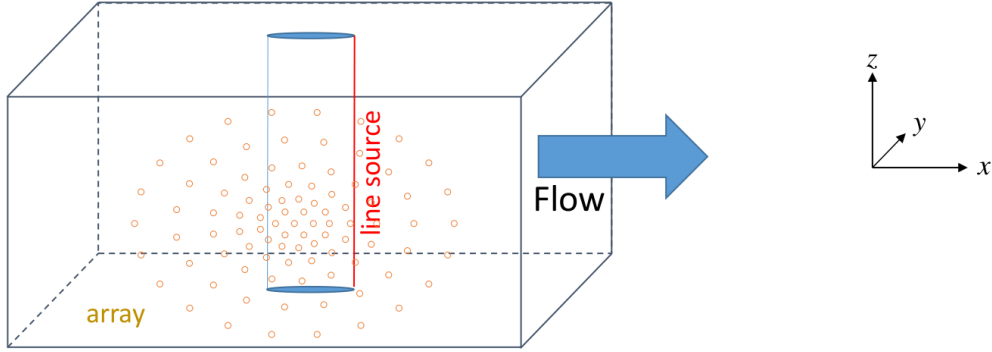


Figure 5. Geometry of the line source benchmark.

## IV. Case: line source

The challenge for this benchmark problem provided by PSA3 is to extract the acoustic signal from a line source out of array measurements that are severely affected by incoherent noise. This is typically the difficulty with measurements of trailing edge noise (e.g., from wind turbine blade sections) in a closed wind tunnel test section with microphones mounted flush in a wall, where sound measurements are hampered by boundary layer turbulence. The geometry of this benchmark can be imagined as a large wind tunnel with  $2 \times 2 \text{ m}^2$  cross-section, capable of testing full-size wind turbine blades, see Fig. 5.

### A. Case description

#### 1. Geometry

A line source of 2 m length was simulated through the origin of a Cartesian coordinate system  $(x, y, z)$ , between  $z = -1 \text{ m}$  and  $z = +1 \text{ m}$ . A uniform flow in the x-direction was modeled at Mach number  $M = 0.22$ . The microphone array, which consisted of 93 microphones, was situated in the plane  $y = -1 \text{ m}$ . The diameter of the array was 1.8 m. The simulations were carried out without the presence of (hard) tunnel walls.

A scan grid of potential sources was not prescribed for this benchmark.

#### 2. Signal

The line source at  $\vec{\xi} = (\xi, \eta, \zeta)$ , with  $\xi = \eta = 0 \text{ m}$ ,  $-z_0 \leq \zeta \leq z_0$ ,  $z_0 = 1 \text{ m}$ , consisted of a very large number of incoherent point sources, at equal spacing and equal strengths. Each individual source corresponded with the free-field Green's function of the convective Helmholtz equation, i.e., with the solution  $p$  of

$$\nabla^2 p - \left( ik + M \frac{\partial}{\partial x} \right)^2 p = \sigma \delta(\vec{x} - \vec{\xi}). \quad (1)$$

Herein,  $\delta$  is the Dirac-delta function,  $\sigma$  the source amplitude, and  $k$  the wave number:  $k = 2\pi f/c$ , with  $f$  the frequency and  $c$  the speed of sound. The solution of (1) is

$$p(\vec{x}) = \frac{-\sigma}{4\pi\tilde{r}(\vec{x}, \vec{\xi})} \exp\left(-\frac{ik}{\beta^2} \left(-M(x - \xi) + \tilde{r}(\vec{x}, \vec{\xi})\right)\right) \\ \text{with } \tilde{r}(\vec{x}, \vec{\xi}) = \sqrt{(x - \xi)^2 + \beta^2((y - \eta)^2 + (z - \zeta)^2)}, \beta^2 = 1 - M^2. \quad (2)$$

For a row of point sources at  $\xi_l = (0 \text{ m}, 0 \text{ m}, \zeta_l)$ , we have

$$p(\vec{x}) = \frac{-\sigma}{4\pi} \exp\left(\frac{ik}{\beta^2} Mx\right) \sum_{l=1}^L \frac{1}{\tilde{r}_l(\vec{x})} \exp\left(-\frac{ik}{\beta^2} \tilde{r}_l(\vec{x})\right) \text{ with } \tilde{r}_l(\vec{x}) = \sqrt{x^2 + \beta^2 (y^2 + (z - \zeta_l)^2)}. \quad (3)$$

Since the sources are incoherent, the following expressions are obtained for the cross-powers between microphones located in  $\vec{x}_m = (x_m, y, z_m)$  and  $\vec{x}_n = (x_n, y, z_n)$ , both with  $y = -1 \text{ m}$ :

$$C_{mn} = \frac{1}{2} pp^* = \frac{|\sigma|^2}{2(4\pi)^2} \exp\left(-\frac{ik}{\beta^2} (-M(\vec{x}_m - \vec{x}_n))\right) \sum_{l=1}^L \frac{1}{\tilde{r}_{l,m} \tilde{r}_{l,n}} \exp\left(-\frac{ik}{\beta^2} (\tilde{r}_{l,m} - \tilde{r}_{l,n})\right) \\ \text{with } \tilde{r}_{l,m} = \sqrt{x_m^2 + \beta^2 (\Delta y^2 + (z_m - \zeta_l)^2)}, \Delta y = 1 \text{ m}. \quad (4)$$

For many closely spaced sources, this can be approximated by an integral

$$C_{mn} = \frac{A}{(4\pi)^2} \exp\left(-\frac{ik}{\beta^2} (-M(\vec{x}_m - \vec{x}_n))\right) \int_{-z_0}^{z_0} \frac{1}{\tilde{r}_m(\zeta) \tilde{r}_n(\zeta)} \exp\left(-\frac{ik}{\beta^2} (\tilde{r}_m(\zeta) - \tilde{r}_n(\zeta))\right) d\zeta \\ \text{with } \tilde{r}_m = \sqrt{x_m^2 + \beta^2 (\Delta y^2 + (z_m - \zeta)^2)}, \Delta y = 1 \text{ m}. \quad (5)$$

where  $\frac{|\sigma|^2}{2}$  is replaced by  $Ad\zeta$ ,  $A$  being the source strength per unit length. For auto-powers ( $m = n$ ), the integral in (5) can be evaluated analytically:

$$C_{mn} = \frac{A}{(4\pi)^2} \int_{-z_0}^{z_0} \frac{d\zeta}{x_m^2 + \beta^2 (\Delta y^2 + (z_m - \zeta)^2)} \quad (6)$$

$$= \frac{A}{(4\pi)^2 \beta^2 \sqrt{\Delta y^2 + \left(\frac{x_m}{\beta}\right)^2}} \left( \arctan\left(\frac{z_0 - z_m}{\sqrt{\Delta y^2 + \left(\frac{x_m}{\beta}\right)^2}}\right) + \arctan\left(\frac{z_0 + z_m}{\sqrt{\Delta y^2 + \left(\frac{x_m}{\beta}\right)^2}}\right) \right) \quad (7)$$

At the center of the array, where  $x_m = z_m = 0 \text{ m}$  we have (since  $\Delta y = z_0 = 1 \text{ m}$ ):

$$C_{mn} = \frac{A}{(4\pi)^2 \beta^2 \Delta y} \frac{\pi}{2} = \frac{A}{32\pi \beta^2 \Delta y} \quad (8)$$

Hence, if  $A = 1 \text{ Pa}^2\text{m}$ , the sound pressure level  $L$  at the array center is 74.17 dB.

For the benchmark,  $A$  was chosen such that

$$10 \lg C_{mn} = 71.16 - \left( 10 - 0.34127 \frac{f}{f_0} - 0.87242 \left(\frac{f}{f_0}\right)^2 + 0.16300 \left(\frac{f}{f_0}\right)^3 - 0.0082341 \left(\frac{f}{f_0}\right)^4 \right) \quad (9)$$

with  $f_0 = 1000 \text{ Hz}$ .

### 3. Noise

On top of the line source induced CSM, a CSM due to white noise was added. For that purpose, 60 seconds of Gaussian white noise were generated at 51.2 kHz sampling rate, incoherent from microphone to microphone. Spectral data were obtained by means of FFT on blocks of 1024 samples, using the energy-preserving Hanning window. Auto- and cross-spectra were averaged over the entire 60 s, using 50% overlapping FFT blocks.

The RMS-value of the synthesized white noise was set at 10 Pa. Consequently, at the individual frequency bands ( $f_j = j\Delta f$ ), the RMS-value is  $10/\sqrt{512} \text{ Pa}$ . The corresponding sound pressure level is 86.89 dB. The signal-to-noise ratio (SNR) varied between -25.7 dB at the lowest frequency (50 Hz) to -15.7 dB at the highest frequency (10 kHz).

Through ensemble averaging, the expected SNR of the cross-spectra increases by  $5 \log(K)$ , where  $K$  is the number of averages. With the above-mentioned signal processing parameters, the number of averages is 6000, implying an increase of 18.9 dB. Consequently, even after removal of the CSM diagonal, the array data contain more noise than signal. This is a worst-case scenario to study what can be extracted from a severely-contaminated dataset. An experiment should not be designed with this poor of an SNR.

## B. Contributions

Results for this case were contributed by five different groups and for DAMAS, CLEAN-SC, OB, FB, SPI and CMF methods. Tab. 4 gives an overview including the details of parameters chosen for the individual contributions.

## C. Results

The results are shown in Fig. 6. Each of these figures includes the noise and the (target) signal spectrum. DAMAS spectra, shown in Fig. 6(a), vary from very poor to quite good. The NASA results highlight the significant effect that CSM diagonal removal has for this case, which is illustrated in Fig. 7. Furthermore, these results seem to indicate the importance of reconstructing the CSM diagonal. However, BTU results are also quite good without reconstructing the CSM diagonal, but using more iterations.

The CLEAN-SC results, shown in Fig. 6(b), do not look very good. Apparently, the high noise levels in the cross-spectra have a negative effect on the identification of coherent sources. The results show again that different implementations of the same method may yield different results.

The SPI spectra (Fig. 6(c)), which were obtained without applying an integration threshold, are very close to the exact solution. This is remarkable in view of the low complexity of the method.<sup>11</sup> The good performance of SPI can, however, be explained by considering the TUD results. TUD did not directly apply SPI, but solved a Least Squares minimization problem to find the best match between the CSM without diagonal and a line source of unknown strength. This approach, which is basically CMF with a single unknown parameter, yields the best solution (in the  $L_2$ -sense). The minimization problem can be solved explicitly, yielding an expression which is almost equal to SPI without the integration threshold.

It must be noted that the quality of SPI depends on the width of the integration sector. This is illustrated by TUD results shown in Fig. 6(d). However, the dimensions of this benchmark case should allow for full size wind turbine blades, for which the frequencies of interest do not exceed 4 kHz. Then, 400 mm width is more than enough to cover the length of trailing edge devices and still acceptable for integration.

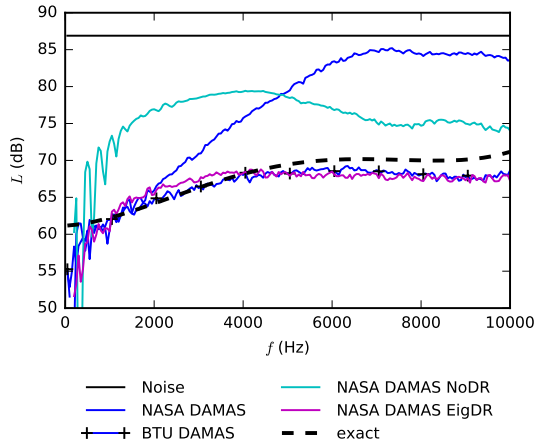
Finally, in Fig. 6(e), results are shown of other beamforming methods: OB and CMF by BTU, and FB by TU Delft. In the figure, FB shows the best agreement with the exact spectrum. However, this may be a ‘‘lucky shot’’. The results were obtained without diagonal removal. FB results in which fractions of the CSM diagonal were removed were significantly different. OB requires a good separation between signal- and noise-related eigenvalues, but the SNR in this benchmark case seems to be too low for that. CMF suffers from the assumption of point sources, which is a poor model in this case.

## V. Conclusion

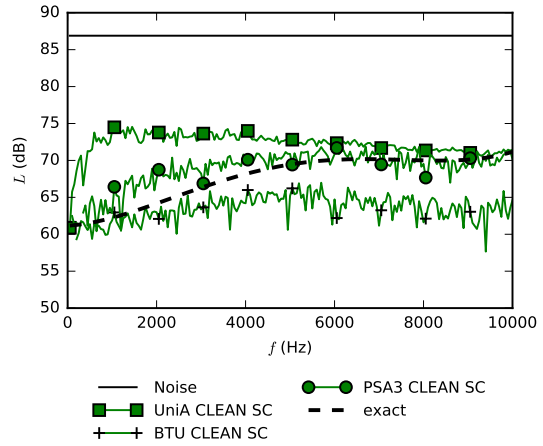
The present paper describes the results from a benchmarking exercise for microphone array methods using synthesized input data. Results are presented for two different cases showing considerable differences between individual methods. For a simple four source scenario with no extra noise, most submitted results are within an error margin of approximately 1 dB. Some method-specific deviations exist. In addition to these, implementation-specific errors manifest themselves for weak sources. Errors that are specific to a certain method and such errors that result from the implementation can be observed to have a considerable impact, especially for the second case which is the line source with strong background noise. For the line source benchmark case, with its low SNR, SPI (without integration threshold) shows the best agreement with the exact results. Overall, it can be concluded that it seems to be well worth further exploring the capabilities of the different methods and also to align the behavior of different implementations of the same method.

Table 4. Overview of contributions for line source case (all dimensions in meters).

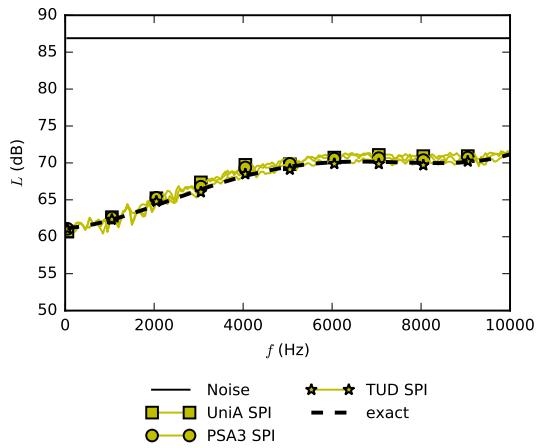
Contributor and method	Parameters	integration sector (rectangular)
NASA DAMAS	number of iteration passes: 200 CSM diagonal removal grid: $2 \times 2.2$ , resolution 0.02	$0.12 \times 2$
NASA DAMAS EigDR	number of iteration passes: 200 CSM eigenvalue based diagonal reconstruction grid: $2 \times 2.2$ , resolution 0.02	$0.12 \times 2$
NASA DAMAS NoDR	number of iteration passes: 200 no CSM diagonal removal grid: $2 \times 2.2$ , resolution 0.02	$0.12 \times 2$
BTU DAMAS	number of iteration passes: 500 CSM diagonal removal grid: $0.8 \times 2.2$ , resolution 0.025	$0.2 \times 2$
BTU CLEAN-SC	damping: 0.6 CSM diagonal removal grid: $0.8 \times 2.2$ , resolution 0.025	$0.2 \times 2$
UniA CLEAN-SC	damping: 0.99 CSM diagonal removal grid: $2 \times 2$ , resolution 0.02	$0.08 \times 2$
PSA3 CLEAN-SC	damping: 0.5 CSM diagonal removal grid: $2 \times 2$ , resolution 0.02	$0.08 \times 2$
BTU OB	source count: 16 CSM diagonal removal grid: $0.8 \times 2.2$ , resolution 0.025	$0.2 \times 2$
BTU CMF	model: uncorrelated point sources solver: NNLS CSM diagonal removal grid: $0.8 \times 2.2$ , resolution 0.025	$0.2 \times 2$
UniA SPI	CSM diagonal removal grid: $2 \times 2$ , resolution 0.02	$0.08 \times 2$
PSA3 SPI	model: line source CSM diagonal removal grid: $2 \times 2$ , resolution 0.02	$0.08 \times 2$
TUD SPI	model: line source CSM diagonal removal grid: $2 \times 2$ , resolution 0.01	$0.04 \times 2$ (and other, see text)
TUD FB	$\nu$ parameter: 50 no CSM diagonal removal grid: $2 \times 2$ , resolution 0.01	$0.1 \times 2$



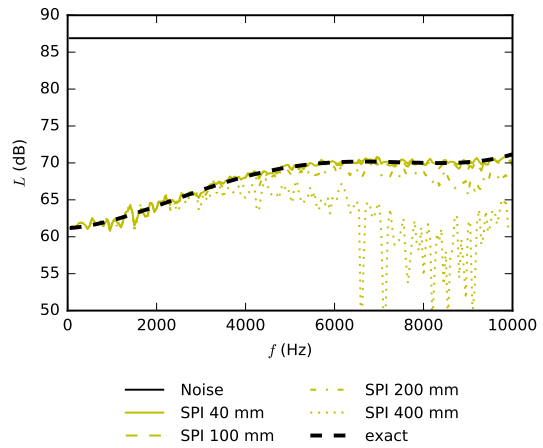
(a) DAMAS results



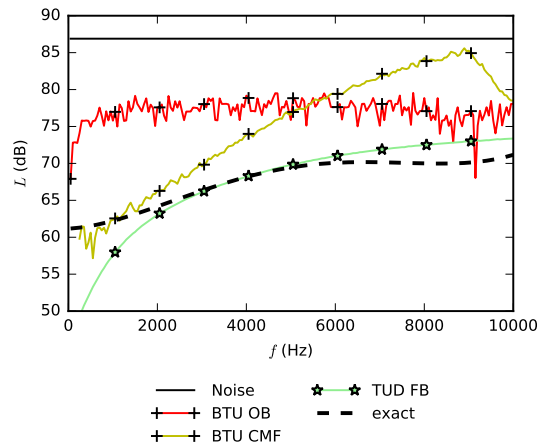
(b) CLEAN-SC results



(c) SPI results



(d) SPI results, different integration sector widths



(e) results for other methods

Figure 6. Results for the line source case.

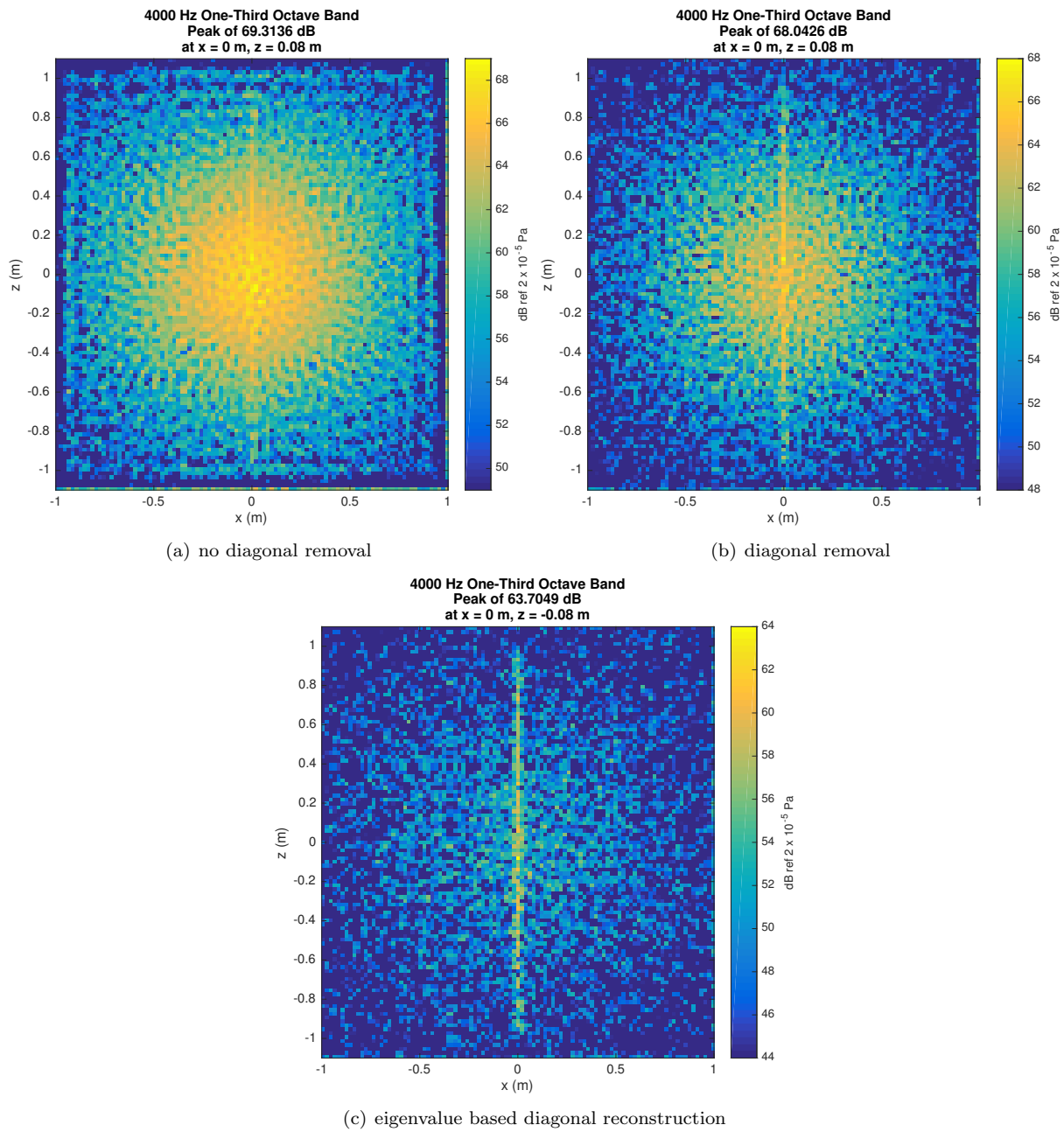


Figure 7. NASA DAMAS sound maps for the line source case.



## References

- <sup>1</sup>Bahr, C. J., Humphreys Jr., W. M., Ernst, D., Ahlefeldt, T., Spehr, C., Pereira, A., Leclère, Q., Picard, C., Porteous, R., Moreau, D. J., Fischer, J., and Doolan, C. J., “A Comparison of Microphone Phased Array Methods Applied to the Study of Airframe Noise in Wind Tunnel Testing,” *23rd AIAA/CEAS Aeroacoustics Conference, AIAA Aviation 2017, Denver, CO, June 2017*, 2017.
- <sup>2</sup>Sarradj, E. and Herold, G., “A Python framework for microphone array data processing,” *Applied Acoustics*, Vol. 116, 2017, pp. 50–58.
- <sup>3</sup>Brooks, T. F. and Humphreys, W. M., “A Deconvolution Approach for the Mapping of Acoustic Sources (DAMAS) Determined from Phased Microphone Arrays,” *Proceedings of the 10th AIAA/CEAS Aeroacoustics Conference, AIAA paper 2004-2954*, 2004.
- <sup>4</sup>Sijtsma, P., “CLEAN based on Spatial Source Coherence,” *Proceedings of the 13th AIAA/CEAS Aeroacoustics Conference, AIAA paper 2007-3436*, 2007.
- <sup>5</sup>Sarradj, E., “A fast signal subspace approach for the determination of absolute levels from phased microphone array measurements,” *Journal of Sound and Vibration*, Vol. 329, 2010, pp. 1553–1569.
- <sup>6</sup>Dougherty, R., “Functional Beamforming,” *Proceedings on CD of the 5th Berlin Beamforming Conference, 19-20 February 2014*, GfAI, Gesellschaft zur Förderung angewandter Informatik e.V., Berlin, February 2014.
- <sup>7</sup>Yardibi, T., Li, J., Stoica, P., Zawodny, N., and Cattafesta III, L., “A covariance fitting approach for correlated acoustic source mapping,” *The Journal of the Acoustical Society of America*, Vol. 127, 2010, pp. 2920.
- <sup>8</sup>Sijtsma, P. and Stoker, R., “Determination of Absolute Contributions of Aircraft Noise Components Using Fly-over Array Measurements,” *Proceedings of the 10th AIAA/CEAS Aeroacoustics Conference, AIAA paper 2004-2958*, 2004.
- <sup>9</sup>Malgoezar, A. M., Snellen, M., Merino-Martinez, R., Sijtsma, P., and Simons, D. G., “On the use of Global Optimization Methods for Acoustic Source Mapping,” *The Journal of the Acoustical Society of America*, Vol. 141, 2017, pp. 453.
- <sup>10</sup>Sarradj, E., “Three-Dimensional Acoustic Source Mapping with Different Beamforming Steering Vector Formulations,” *Advances in Acoustics and Vibration*, Vol. 2012, No. 292695, 2012, pp. 1–12.
- <sup>11</sup>Brooks, T. and Humphreys, W., “Effect of Directional Array Size on the Measurement of Airframe Noise Components,” *Proceeding of the 5th AIAA/CEAS Aeroacoustics Conference, AIAA paper 99-1958*, 1999.